

Nonlinear Behavior of Unidirectional and Angle Ply Laminates

R. S. Sandhu*

Air Force Flight Dynamics Laboratory, Wright-Patterson Air Force Base, Ohio

An analytical technique relating the response to failure of unidirectional off-axis and angle ply laminates to the behavior of laminae under simple load conditions is presented. In the technique, cubic spline interpolation functions are used to represent experimentally obtained stress-strain data. These data, in conjunction with incremental constitutive relations and concepts of laminated plate theory, are employed to predict the behavior of laminates under incremental loading. The onset of the failure condition is determined using a failure criterion which is a function of both stress and strain states. The available experimental data are compared not only with predictions based upon the present theory, but also with the theoretical results obtained using the techniques of Petit and Waddoups and of Hahn. It is shown that experimental results agree most closely with the stress-strain curves based upon the present theory than those obtained by the other two techniques.

Nomenclature

$[A]$	= stiffness matrix of the laminate
$[A]^{-1}$	= compliance matrix of the laminate
B	= ratio of stress increments
$[C]_k$	= stiffness matrix of the k th ply relative to the material axes 1, 2
$[\bar{C}]_k$	= stiffness matrix of the k th ply relative to the laminate axes X, Y
$i, j (i, j = 1, 2, 3)$ $(i = 1, 2, 6)$	= indices
K, K_{ij}, K_1, K_2, K_6	= material characteristic
k_j	= number associated with a reference ply in a laminate
$m_{ij} (i, j = 1, 2, 3)$ m_1, m_2, m_6	= indices associated with strain energy functions
$[dN]$	= increment of stress resultants
n	= stress increment cycle
p	= total number of plies in the laminate
S_{6666}	= constant
$S_{ijrs}, S_{ij}, [S]$	= elements of the compliance matrix of the ply
$r, s, (r, s = 1, 2, 3)$	= indices
T	= transformation matrix relating the material axes 1, 2, and the laminate axes X, Y
X, Y	= laminate coordinate axes
α	= angle between the load and the major material axis 1
$d\epsilon_{ij}, d\epsilon_i, [d\epsilon]$	= increments of the strain component of the ply
$[d\bar{\epsilon}], [d\bar{\epsilon}^\circ]$	= increments of the strain components of the laminate
$\hat{\epsilon}_{ij}, \hat{\epsilon}_1, \hat{\epsilon}_2, \hat{\epsilon}_6$	= current strain components of the ply
ϵ_{iu}	= ultimate strain components of the ply in simple loading
ϵ_6	= shear strain in a ply
ν_{12}, ν_{21}	= major and minor Poisson ratios
$d\sigma_{ij}, d\sigma_j, [d\sigma]$	= increments of the stress components of the ply
σ_6	= shear stress in the ply
$1, 2$	= material axes of the ply

I. Introduction

FILAMENTARY composite laminates are being used in aircraft structural components in increasing numbers. For the design to be satisfactory, it is essential to determine the stress-strain behavior and the ultimate strength of the laminates. This can be accomplished experimentally, but such a procedure is both expensive and inconvenient, considering the variety of laminates which can be fabricated. The other technique is to relate analytically the properties of the lamina to those of laminates. This method has been the subject of many studies.¹⁻⁹ In all of these studies, the lamina stress-strain response under simple loading conditions (uniaxial tension and compression along and transverse to the material axes and shear to failure) forms the basis.

In early attempts,¹⁻⁴ linearity of stress-strain response was assumed even though tests indicated significant nonlinear behavior of the composite lamina under transverse and shear loadings. Later on this restriction of linearity was relaxed.⁵⁻⁹ Petit and Waddoups used a piecewise linear representation of the stress-strain curves. The loading is proportional and is applied in small increments to compute the current stress-strain states. In this method biaxial lamina strains are used to obtain tangent moduli from stress-strain data generated under simple load conditions. Hahn⁶ proposed a method which allows only for the nonlinearity of shear stress-strain response by an equation

$$\epsilon_6 = S_{66}\sigma_6 + S_{6666}\sigma_6^3 \quad (1)$$

where σ_6, ϵ_6 are shear stress and shear strain and S_{66}, S_{6666} are constants. In this approach no distinction is made between tensile and compressive behaviors of the lamina, and problems of failure are not dealt with. Hashin et al.⁸ used Ramberg-Osgood parameters to represent the nonlinear response of the lamina subjected to transverse and shear loads. This representation of nonlinear response is similar to Eq. (1). The behavior in the direction of fibers is assumed to be linear. The failure of the lamina is based on either the stress along the fibers exceeding a limit or the tangent modulus attaining a value less than a specified one.

The technique described below uses piecewise cubic spline interpolation functions¹⁰⁻¹³ to represent the basic stress-strain data. Cubic spline functions are simple to use. They yield smooth composite stress-strain curves from which accurate moduli of elasticity over the entire range of the curves can be determined. This quality is especially desirable in the iterative procedure used in this technique. An incremental constitutive equation is used to relate the increments of stresses and strains. Using the basic data, and the constitutive relations, the ultimate cumulative response of the laminate under in-

Submitted March 29, 1974; presented as Paper 74-830 at the AIAA/ASME/SAE 15th Structures, Structural Dynamics and Materials Conference, Las Vegas, Nev., April 17-19, 1974; revision received April 7, 1975.

Index category: Structural Composite Materials (including Coating).

*Aerospace Engineer, Design and Analysis Branch, Structures Division.

cremental loading is determined by plywise application of a new failure criterion. This criterion is based upon the concept that strain energies under longitudinal, transverse, and shear loadings are independent parameters. The analytical response obtained by three methods (the proposed technique and those of Refs. 5-7) is compared with the available experimental results.

II. Method of Analysis

To define the general incremental constitutive relationship for anisotropic materials, it is assumed that a) the increment of strain depends upon the strain state and the increment of stress; and 2) the increment of strain is proportional to the increment of stress. Using these assumptions, the incremental constitutive law can be written as

$$d\epsilon_{ij} = S_{ijrs}(\epsilon_{ij}) d\sigma_{rs} \quad (i,j,r,s=1,2,3) \quad (2)$$

where $d\epsilon_{ij}$, $d\sigma_{rs}$ are strain and stress increments and S_{ijrs} is a function of strains ϵ_{ij} .

The incremental constitutive relation using contracted notation for the lamina under generalized plane stress reduces to

$$d\epsilon_i = S_{ij}(\epsilon_i) d\sigma_j \quad (i,j=1,2,6) \quad (3)$$

Assuming that the lamina remains orthotropic at all load levels, Eq. (3) can be written as

$$\begin{bmatrix} d\epsilon_1 \\ d\epsilon_2 \\ d\epsilon_6 \end{bmatrix} = \begin{bmatrix} S_{11} & S_{12} & S_{16} \\ S_{21} & S_{22} & S_{26} \\ S_{61} & S_{62} & S_{66} \end{bmatrix} \begin{bmatrix} d\sigma_1 \\ d\sigma_2 \\ d\sigma_6 \end{bmatrix} \quad (4)$$

or simply

$$[d\epsilon] = [S] [d\sigma] \quad (5)$$

where

- $d\sigma_1, d\epsilon_1$ = normal stress and strain increments in the fiber direction
- $d\sigma_2, d\epsilon_2$ = normal stress and strain increments in the transverse directions
- $d\sigma_6, d\epsilon_6$ = shear stress and strain increments
- $S_{11}, S_{12}, \text{etc.}$ = elements of compliance matrix representing the average values during the increment of stresses

Experimental results presented in Sec. IV indicated that the assumption about orthotropic behavior of the lamina is reasonable.

In the application of the incremental constitutive law to multidirectional laminates, Eq. (5) for the k th ply is written as

$$[d\sigma]_k = [C]_k [d\epsilon]_k \quad (6)$$

where

- $[C]_k = [S]_k^{-1}$ = stiffness matrix of the k th ply
- $[d\sigma]_k$ = stress increment in the k th ply relative to the material axes, 1,2
- $[d\epsilon]_k$ = strain increment in the k th ply relative to material axes 1,2

The material axes 1,2 coincide with fiber and transverse directions, respectively. In the case of multidirectional laminates, load axes X, Y generally do not coincide with the material axes 1,2. Stress and strain increments in two-coordinate systems are related by a transformation matrix $[T]_k$, i.e.,

$$[d\sigma]_k = [T]_k [d\bar{\sigma}]_k \quad (7)$$

$$[d\epsilon]_k = [T]_k [d\bar{\epsilon}]_k \quad (8)$$

where $[d\bar{\sigma}]_k$ and $[d\bar{\epsilon}]_k$ are the stress and strain increments in the k th ply relative to the X, Y coordinate system. Substitution of Eq. (7) and (8) in Eq. (6) yields

$$[d\bar{\sigma}]_k = [\bar{C}]_k [d\bar{\epsilon}]_k \quad (9)$$

where

$$[\bar{C}]_k = [T]_k^{-1} [C]_k [T]_k \quad (10)$$

Assuming that stresses are distributed uniformly through the thickness of each ply, the stress resultant increments $[dN]$ in X, Y coordinates are given by

$$[dN] = \sum_{k=1}^p [d\bar{\sigma}]_k t_k \quad (11)$$

where

- t_k = thickness of the k th ply
- p = number of plies in a laminate

Combining Eqs. (9) and (11), the stress resultant increments become

$$[dN] = \sum_{k=1}^p t_k [\bar{C}]_k [d\bar{\epsilon}]_k \quad (12)$$

Assuming that the strain increments are the same for all plies of the laminate, i.e.,

$$[d\bar{\epsilon}]_k = [d\epsilon^\circ] \quad (13)$$

Eq. (12) becomes

$$[dN] = [A] [d\epsilon^\circ] \quad (14)$$

where

$$[A] = \sum_{k=1}^p t_k [\bar{C}]_k \quad (15)$$

Inversion of Eq. (14) yields

$$[d\epsilon^\circ] = [A]^{-1} [dN] \quad (16)$$

In Eq. (16), $[A]^{-1}$ represents average compliance properties of the laminate during the $(n+1)$ th load increment. However, these properties are not known when the $(n+1)$ th load increment is applied. To overcome this difficulty the elastic properties at the end of the n th load increment are used in Eq. (16) to compute the laminate strain increments $[d\epsilon^\circ]$ and stress increments $[d\sigma]_k$ and strain increments $[d\epsilon]_k$ in plies. These stress and strain increments are added to stresses and strains at the n th load increment to obtain the current stresses and strains in the plies. However, the use of strain components ϵ_1 and ϵ_2 in plies under biaxial stresses to determine tangent moduli from stress-strain data generated under simple load conditions is erroneous. For example, ϵ_2 under a biaxial stress (σ_1, σ_2) corresponds to the curve ON (Fig. 1) on the plane $OEHG$, whereas the simple stress-strain curve OM lies on the plane $OEDC$. Since experimental stress-strain data similar on ON are not available, it is assumed that, for each ply, simple equivalent strain increments can be computed from the following expressions (see Ref. 9):

$$d\epsilon_1|_{\text{Eq.}} = d\epsilon_1 / (1 - \nu_{12}B) \quad (17)$$

$$d\epsilon_2|_{\text{Eq.}} = d\epsilon_2 / (1 - \nu_{21}/B) \quad (18)$$

where

$$\nu_{12} = \text{major Poisson's ratio}$$

$$B = d\sigma_2/d\sigma_1$$

Using the strains corrected for simple load conditions, average elastic properties of the plies are determined and a new $[A]^{-1}$ is computed. This procedure is repeated until the difference between values of $[d\epsilon^\circ]$ in two consecutive cycles is reduced to the order of approximation desired. The repetitive use of the procedure just outlined generates the response of the laminates.

III. Failure Criterion

Under incremental loading the laminas reach a state when they can no longer sustain additional loads. Determination of this failure condition under general stress states is accomplished by a criterion. The criterion relates this failure to the failure conditions of the laminas determined under simple loadings. In these criteria for anisotropic materials, yield and ultimate states are assumed analogous.¹⁴ For materials exhibiting nonlinear behavior, the two states are not the same, and the failure state would depend upon both stresses and strains. A scalar function f defining the failure criterion of materials exhibiting nonlinear behavior can be written as

$$f(\sigma, \epsilon, K) = 1 \quad (19)$$

where σ, ϵ , are stress and strain states and K represent material characteristics.

A simple scalar function dependent upon both stress and strain states is the strain energy of the material exhibiting nonlinear behavior. In the case of an orthotropic material, strain energies, under uniaxial tension and compression along and transverse to the material axes, and shear are independent parameters. To measure the level of the effect of both stress and strain states on the orthotropic materials under a combined stress state, a simple scalar function is a linear combination of functions of different strain energies. In this form it can be written as

$$\sum_{i=1}^3 \sum_{j=1}^3 K_{ij} \left[\int_{\epsilon_{ij}} \sigma_{ij} d\epsilon_{ij} \right]^{m_{ij}} = 1 \quad (20)$$

where ϵ_{ij} are the current strain components and m_{ij} are the parameters defining the shape of the failure surface in the strain-energy space. The failure criterion is based upon total strain energies. It includes the effect of hydrostatic loading. This inclusion is necessary to allow for the heterogeneous deviatoric stress field caused in fiber-reinforced composites by the hydrostatic loading.¹⁵

Equation (20), using contracted notation, and specialized for the plane stress condition, becomes

$$K_1 \left[\int_{\epsilon_1} \sigma_1 d\epsilon_1 \right]^{m_1} + K_2 \left[\int_{\epsilon_2} \sigma_2 d\epsilon_2 \right]^{m_2} + K_6 \left[\int_{\epsilon_6} \sigma_6 d\epsilon_6 \right]^{m_6} = 1 \quad (21)$$

Using the results of tests under simple load conditions,

$$K_i = \left[\int_{\epsilon_{iu}} \sigma_i d\epsilon_i \right]^{-m_i} \quad (i=1, 2, 6) \quad (22)$$

where ϵ_{iu} are the ultimate normal (tensile or compressive) and shear strains. The shape of the failure surface [Eq. (21)] in the strain-energy space is determined by the shape factor, m_i . For $m_1 = m_2 = m_6 = m = 2$, it is spherical and for $m_1 = m_2 = m_6 = m = 1$, it is a pyramidal surface.

This criterion for three values of the parameter m , namely, $m = 1/2, 1$, and 2 , is compared with some of the other failure theories for boron-epoxy material systems. The comparison is confined to the first quadrant of the stress space (Fig. 2). At present there are no reliable experimental data for boron-epoxy unidirectional laminas under biaxial stress states which

could be used to determine suitable values of m_1, m_2 , and m_6 . For the study reported herein, $m_1 = m_2 = m_6$ is taken to be unity. In this form the three terms of Eq. (21) are the ratios of current energy levels (due to longitudinal, transverse, and shear loading) to the maximum available ones. When the sum of the three ratios equals unity, the lamina degrades completely, and the three ratios at that time are contributions to degradation made by longitudinal, transverse, and shear stresses acting on the lamina.

IV. Analytical-Experimental Correlation

There are four methods which account for some form of nonlinearity of the lamina stress-strain curves. For the purpose of analytical-experimental correlation, however, only three techniques (Hahn, Petit and Waddoups, and the present approach) have been used. In Hahn's method only the shear stress-strain behavior of the lamina is assumed to be nonlinear. The use of Eq. (1) to approximate the nonlinear shear curve is too restrictive. The other two techniques are similar in some respects but differ in others. They are compared in the following paragraphs:

1) Both methods allow all of the lamina stress-strain curves to be nonlinear. Petit and Waddoups use a piecewise linear representation, whereas the present method employs piecewise cubic spline functions. The latter provides not only a more accurate representation of the lamina curves using fewer data points but also permits easy use of a predictor-corrector and iterative approach to determine laminate behavior under incremental loading.

2) In the Petit-Waddoups technique it is assumed that the tangent modulus relative to one material axis is not influenced by the presence of stresses in the other directions. If the lamina stress-strain curves are highly nonlinear, this assumption has a significant effect upon the laminate stress-strain response. For example, if the longitudinal lamina stress is tensile and the transverse stress is compressive, the longitudinal tangent modulus will be less than the one when there is no transverse stress. This situation is reversed if the transverse stress is tensile. However, in the present technique the effect of the presence of transverse stresses is allowed for in the determination of the tangent moduli.

3) Both methods use lamination theory to generate the laminate compliance which is used to compute laminate strain increments under the applied stress increment. These laminate strain increments are added to those obtained previously to determine current strains. In the Petit-Waddoups technique these strains are used to compute the laminate compliance for the next load increment. This technique is essentially a predictor type. In the present analysis, the strains are used to determine average laminate compliance for the same load increment, and a new set of laminate strains are obtained. This procedure is repeated until the difference between two consecutive sets of laminate strains is less than the prescribed value.

The difference between this predictor-corrector and iterative technique and that of Petit and Waddoups is illustrated in Fig. 3. Figure 3 indicates the relationship of the response under uniaxial loading of a $\pm 45^\circ$ laminate to that of the lamina. Although, for the sake of clarity, only the shear stress-strain curve of the lamina is shown in Fig. 3, the effects of longitudinal and transverse stress-strain curves have been allowed for in the laminate behavior. Using the laminate compliance corresponding to the point 0 of the lamina curves, the laminate strain increment for a stress increment of 12 ksi is computed. It yields a total axial-laminate strain ϵ_{x1} . In the case of Petit and Waddoups, the strain ϵ_{x1} is used to determine lamina strains γ_1 , etc., to compute laminate compliance for the next load increment. In the present approach, a new laminate compliance corresponding to the lamina point A (average of γ_0 and γ_1 , etc.) is computed to yield a laminate strain ϵ_{x2} . This procedure is repeated for the lamina point B, etc., until the difference between two values of the laminate

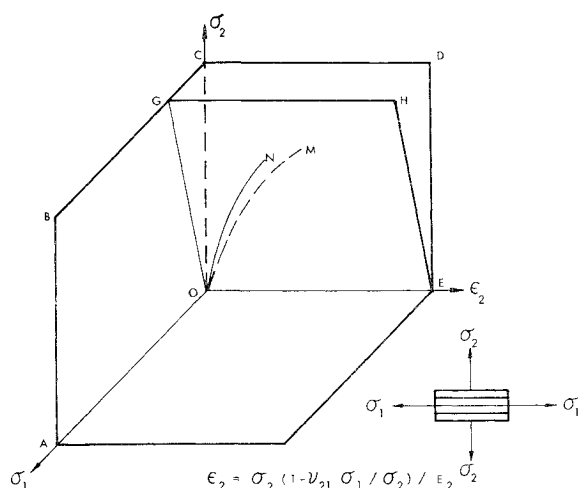
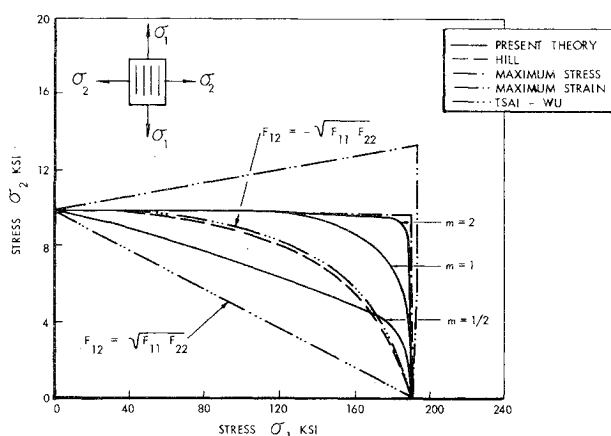
Fig. 1 Strain (ϵ_2) vs biaxial stress field (σ_1, σ_2).

Fig. 2 Comparison of various strength theories.

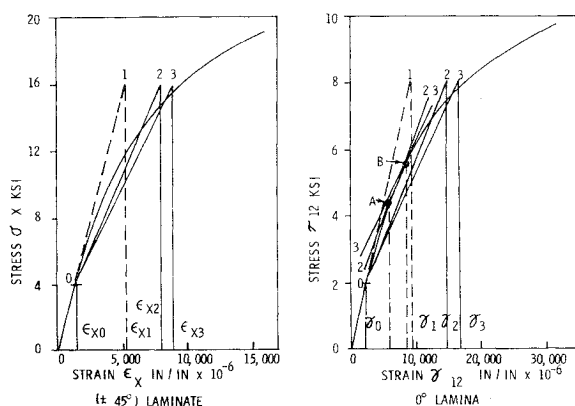


Fig. 3 Lamina-lamina response.

strains is smaller than a predetermined value. It is obvious from Fig. 3 that the laminate stress-strain curve based upon the Petit-Waddoups technique depends upon the size of load increments giving rise to cumulative error. On the other hand, the present approach is practically independent of the size of load increments. In this iterative procedure strains converge rapidly to the correct values.

4) In terms 1-3, the factors influencing the stress-strain response of the laminate under incremental loading were discussed. The incremental loading cannot proceed indefinitely. Presently a stage is reached when a lamina or laminas in the laminate can sustain no more load. This stage is determined by a failure criterion. Petit and Waddoups

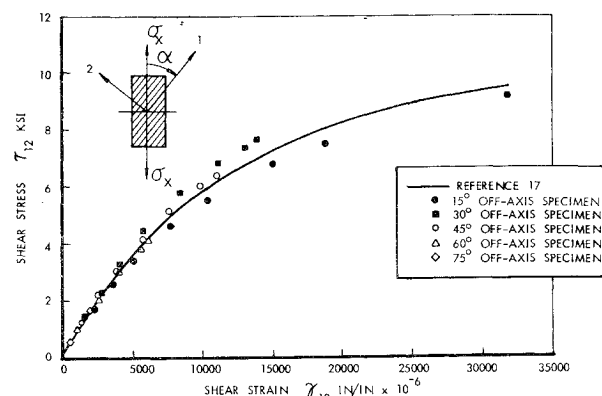


Fig. 4 Lamina shear response.

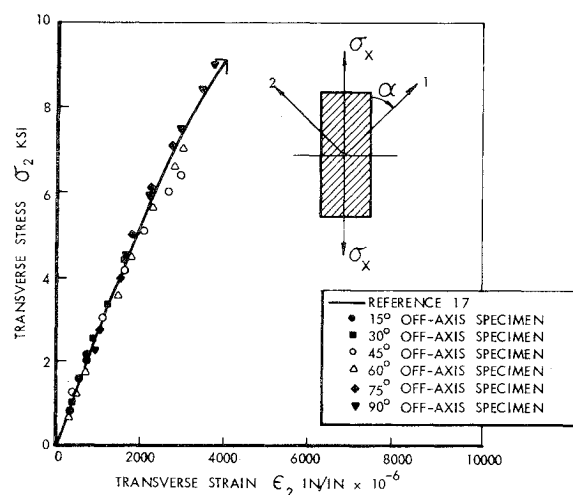


Fig. 5 Lamina transverse tension response.

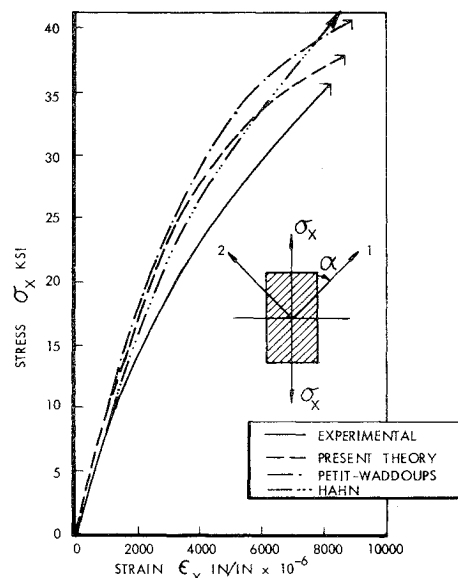


Fig. 6 Boron-epoxy 15° off-axis coupon.

hypothesize that the failure of the lamina occurs when any of the strain components relative to the material axes reaches a limiting value established by simple tests. In this criterion it is assumed tactfully that the strain along one material axis is not influenced by the presence of stresses along other axes. For a tension-tension case, the criterion will yield higher failure stress than stress corresponding to simple load condition. In the case of tension-compression loading, the failure stress

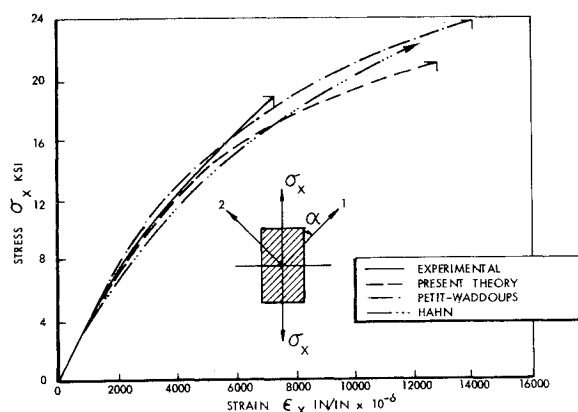


Fig. 7 Boron-epoxy 30° off-axis coupon.

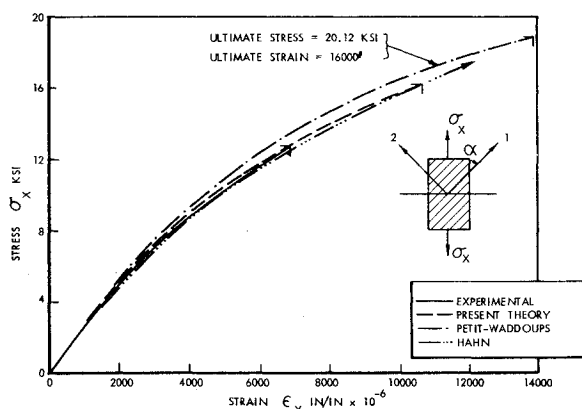


Fig. 8 Boron-epoxy 45° off-axis coupon.

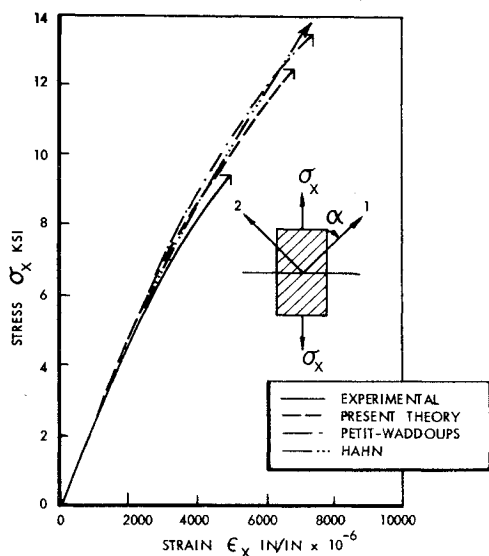


Fig. 9 Boron-epoxy 60° off-axis coupon.

would be lower. In the present approach, the failure condition of the lamina or laminas is determined by using Eq. (21), which allows for all of the stress components. This criterion is new, but rational, for orthotropic materials exhibiting nonlinear behavior. For determining the values of m_1, m_2 , and m_6 , reliable experimental data are required. In the form presented herein, $m_1 = m_2 = m_6 = m = 1$ is assumed.

Experimental data for the purpose of analytical-experimental correlation are obtained using a boron-epoxy material system. The curves obtained under simple load conditions¹⁶ are compared with resolved stress-strain curves (Figs. 4 and 5) of off-axis coupons.¹⁷ The proximity of the

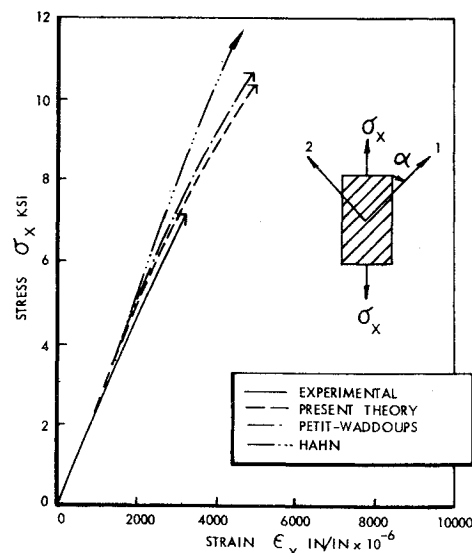
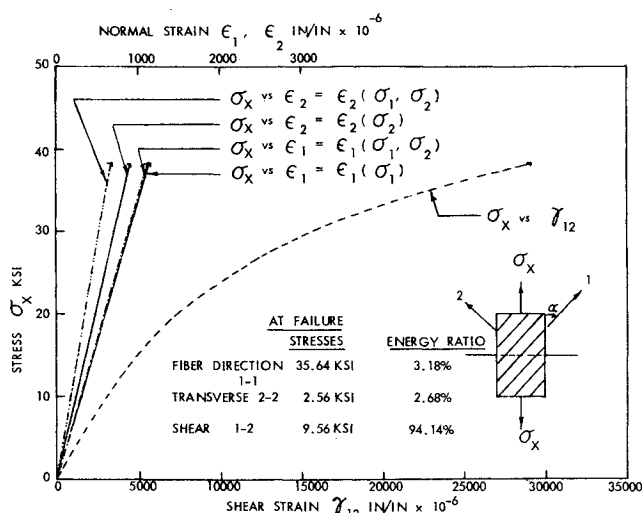


Fig. 10 Boron-epoxy 75° off-axis coupon.

Fig. 11 Stress σ_x vs strains along material axes of 15° boron-epoxy off-axis coupon.

two sets of curves substantiates the premise that the boron-epoxy laminae tend to retain orthotropic characteristics at all load levels, i.e., shear stresses are functions of shear strains, and normal stresses are functions of normal strains only.

A computer program incorporating the concepts of Sec. II and III is utilized to predict the response of off-axis and angle ply laminates. In addition to this, analytical curves are obtained using the method of Ref. 5 (RD5 computer program) and of Refs. 6 and 7.

A. Off-Axis Coupons

Experimental data for unidirectional off-axis boron-epoxy coupons used in the analytical-experimental correlation are taken from Ref. 17. In the experimental program, 0.5-in-wide specimens with an aspect ratio of 16 in the test section were used. Each was instrumented with a strain gage rosette located at the edge of the specimen.

Stress-strain curves for 15°, 30°, 45°, 60°, and 75° off-axis coupons obtained experimentally¹⁷ and using the three analytical techniques are shown in Figs. 6-10. As seen from Fig. 11, the response of the 15° off-axis coupon is determined mainly by the lamina shear stress-strain behavior. The shear effect contributes 94.14% to the total degradation of the coupon. The stiffer shear stress-strain response of the lamina as compared to that of the 15° coupon (Fig. 4) is reflected in

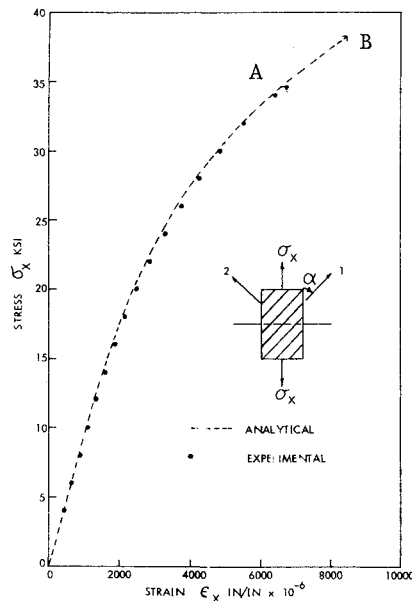


Fig. 12 Boron-epoxy 15° off-axis coupon tested in-house.

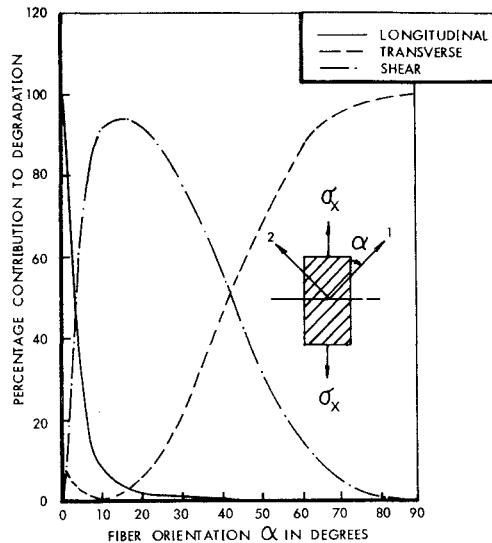
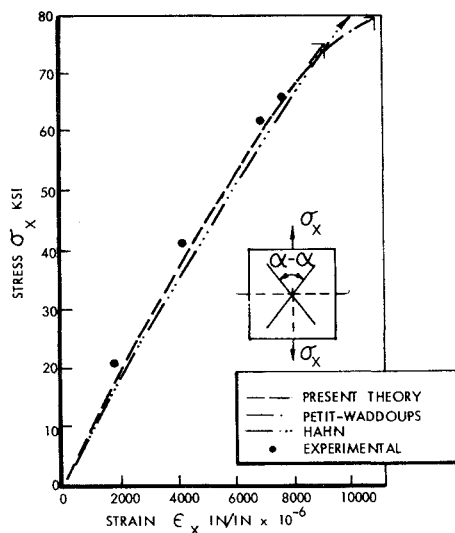
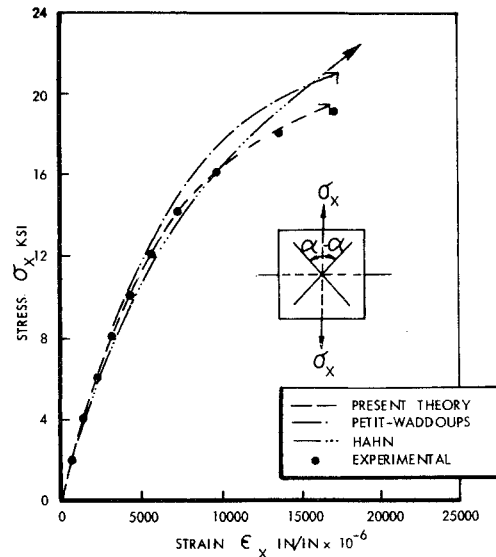
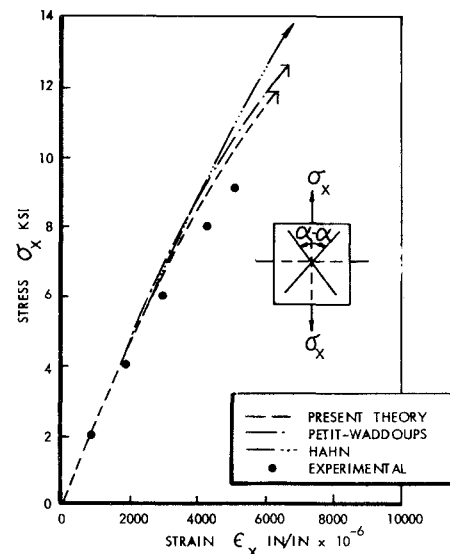


Fig. 13 Percentage contribution to degradation of off-axis specimens.

Fig. 14 Response of $\pm 30^\circ$ laminate subjected to stress σ_x only.Fig. 15 Response of $\pm 45^\circ$ laminate subjected to stress σ_x only.Fig. 16 Response of $\pm 60^\circ$ laminate subjected to stress σ_x only.

the deviation observed between the predicted analytical and experimental response. It probably is due to strain measurements being affected by edge effects. To verify this effect, the 15° off-axis coupon was tested. In this test, strain gage rosettes were located at the center of the midsection of a 1-in. side specimen. The results of the test are shown in Fig. 12. It is seen from the figure that the experimental curve is very close to the curve predicted by using in-house generated basic properties data. However, the experimental strength (point A of Fig. 12) is smaller than the predicted one (point B of Fig. 12). The lower experimental strength is due to the nonuniform stress field in the coupon. To substantiate this premise, the coupon was analyzed using a finite-element technique in conjunction with the concepts of Sec. II and III. The strength of the coupon so obtained was almost identical to the experimental one. Presumably experimental results of 30°, 45°, 60°, and 75° off-axis coupons are affected similarly.

With increasing orientation of fibers, the effect of the lamina transverse stress-strain response on the behavior of off-axis coupons increases, and at the same time the shear effect diminishes. This trend is observed easily in Fig. 13, wherein three energy ratio (longitudinal, transverse, and shear) curves corresponding to failure conditions are shown as percentage contributions to degradation for various fiber

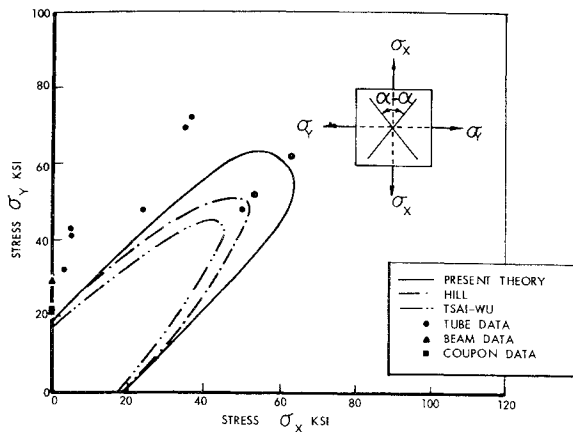


Fig. 17 Strength envelope for $\pm 45^\circ$ laminate.

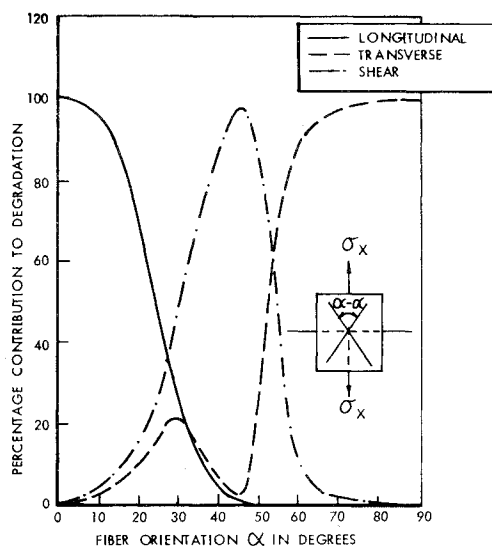


Fig. 18 Percentage contribution to degradation of $\pm \alpha^\circ$ laminates subjected to stress σ_x only.

orientations. These contributions determine the failure modes of the coupons. For orientation angles greater than 60° , the contribution to failure by the transverse effect exceeds 87.97%. Under these conditions the analytical curves (Fig. 9 and 10), based upon Ref. 6, which does not allow for the nonlinearity of the transverse stress-strain of the lamina, deviate more from the experimental behavior. There is a better agreement between the experimental stress-strain curves and the analytical responses based upon the concepts presented here than those of Refs. 5 and 6 (paragraphs 1-3). The difference in the strength predicted by the present technique and that of Ref. 5 is due to reasons discussed earlier. However, experimental and predicted strengths tend to diverge with increasing orientation especially for the fiber orientation greater than 45° . This divergence may be due to the nonuniformity of the stresses in the test section, the width-effect of the specimens, residual stresses, etc.

B. Angle Ply Laminates

In the case of angle ply laminates, the available experimental data required to validate the concepts of Secs. II and III are quite meager. They consist essentially of results for laminates subjected to uniaxial tensile loads. Some experimental strength data from biaxial tests on $\pm 45^\circ$ laminates are reported in Ref. 18. In Figs. 14-16 experimental responses of $\pm 30^\circ$, $\pm 45^\circ$, and $\pm 60^\circ$ laminates¹⁷ subjected to uniaxial loads are compared with the analytical results obtained using

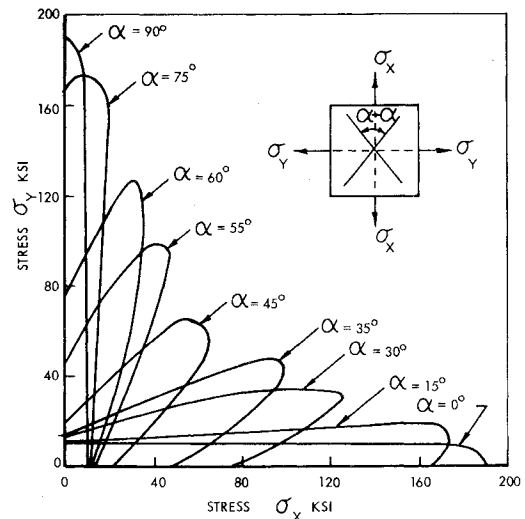


Fig. 19 Strength envelopes for $\pm \alpha^\circ$ laminates.

the present theory and the techniques of Refs. 5 and 7. The experimental stress-strain curves agree more closely with the stress-strain curves based upon the present theory than those using the other two techniques.

Experimental stress-strain plots for $\pm 45^\circ$ laminates subjected to biaxial loading are not available in the literature. Hence no comparison is possible. However, a comparison of predicted and experimental strengths is shown in Fig. 17. The experimental data indicate large scatter, and no definite conclusion can be drawn.

Because of the lack of sufficient experimental data, full corroboration of the proposed analytical technique as applied to angle ply laminates is not feasible, but some insight into their behavior may be obtained from Figs. 18 and 19. It is observed from Fig. 18 that 1) for $\alpha = 0^\circ$ – 30° , longitudinal contribution to degradation decreases, and shear and transverse contributions increase (transverse stresses being compressive); 2) for $\alpha = 45^\circ$, shear contribution reaches a maximum of 97.57%, with longitudinal and transverse contributions being 0.71% and 1.72%; and 3) for $\alpha = 60^\circ$ – 90° , the failure is essentially a transverse failure. In Fig. 19, it is seen that, with increasing fiber orientation, transverse laminate strength tends to increase with decreasing longitudinal strength. The points of maximum curvature on the strength envelopes correspond to the fibers being stressed most highly. In other regions either the transverse or the shear contribution to degradation dominates.

V. Conclusions

It has been shown that the incremental constitutive relations in conjunction with the failure criterion proposed herein provide suitable analytic means for predicting the behavior of off-axis and angle ply laminates under general stress states using only the lamina property data obtained under simple load conditions. This technique easily can be extended to the study of multidirectional laminates with some additional postulates. The study has indicated the need to improve test techniques to eliminate the gray area that exists between theory and experiment.

References

- ¹Tsai, S. W., "Strength Characteristics of Composite Materials," NASA CR-224, April 1965.
- ²Tsai, S., Adams, D. F., and Doner, D. R., "Analysis of Composite Structures," NASA CR-620, Nov. 1966.
- ³Noyes, J. V. and Jones, B. H., "Crazing and Yielding of Reinforced Composites," ARML-TR-68-51, March 1968, Air Force Materials Laboratory, Wright-Patterson Air Force Base, Ohio.

⁴Chiu, K. D., "Ultimate Strength of Laminated Composites," *Journal of Composite Materials*, Vol. 3, July 1969, p. 578.

⁵Petit, P. H. and Waddoups, M. E., "A Method of Predicting the Nonlinear Behavior of Laminated Composites," *Journal of Composite Materials*, Vol. 3, Jan. 1969, p. 2.

⁶Hahn, H. T. and Tsai, S. W., "Nonlinear Elastic Behavior of Unidirectional Composite Laminates," *Journal of Composite Materials*, Vol. 7, Jan. 1973, pp. 102-108.

⁷Hahn, H. T., "Nonlinear Behavior of Laminated Composites," *Journal of Composite Materials*, Vol. 7, April 1973, pp. 257-271.

⁸Hashin, Z., Bagchi, D., and Rosen, B. W., "Nonlinear Behavior of Fiber Composite Laminates," NASA CR-2313, 1973.

⁹Sandhu, R. S., "Ultimate Strength Analysis of Symmetric Laminates," AFFDL-TR-73-137, AD 779927, 1973, Air Force Flight Dynamics Laboratory, Wright-Patterson Air Force Base, Ohio.

¹⁰Schoenberg, I. J., "Contribution to the Problem of Approximation of Equidistant Data by Analytic Functions," *Quarterly of Applied Mathematics*, Vol. 4, 1946, pp. 112-141.

¹¹Ahlberg, J. H., Nilson, E. N., and Walsh, J. L., *Theory of Splines and Their Applications*, Academic Press, New York, 1967.

¹²Walsh, J. L., Ahlberg, J. H., and Nilson, E. N., "Best Approximation Properties of the Spline Fit," *Journal of Mathematics and Mechanics*, Vol. II, March 1962, pp. 225-233.

¹³Ralston, A. and Wilf, H. S., *Mathematical Methods for Digital Computer*, Vol. II, J. Wiley, New York.

¹⁴Sandhu, R. S., "A Survey of Failure Theories of Isotropic and Anisotropic Materials," AFFDL-TR-72-71, AD 756889, Jan. 1972, Air Force Flight Dynamics Laboratory, Wright-Patterson Air Force Base, Ohio.

¹⁵Lin, T. H., Salinas, D., and Ito, Y. M., "Effects of Hydrostatic Stress on the Yielding of Cold Rolled Metals and Fiber Reinforced Composites," *Journal of Composite Materials*, Vol. 6, July 1972, pp. 409-413.

¹⁶McKagne, E. L., Lemon, G. H., and Kaminski, B. E., "Development of Engineering Data for Advanced Composite Materials," AFML-TR-70-108, Vol. 1, 1970, Air Force Materials Laboratory, Wright-Patterson Air Force Base, Ohio.

¹⁷Cole, B. W. and Pipes, R. B., "Filamentary Composite Laminates Subjected to Biaxial Stress Fields," AFFDL-TR-73-115, AD 785362, 1973, Air Force Flight Dynamics Laboratory, Wright-Patterson Air Force Base, Ohio.

¹⁸"Advanced Composite Wing Structures, Boron-Epoxy Design Data, Vol. III—Experimental Data," Contract F33615-68-C-1301, TR AC-SM-ST-8085, Vol. III, Nov. 1967, Grumman Aerospace Corp., Bethpage, N.Y.

From the AIAA Progress in Astronautics and Aeronautics Series . . .

THERMOPHYSICS OF SPACECRAFT AND PLANETARY BODIES; RADIATION PROPERTIES OF SOLIDS AND THE ELECTROMAGNETIC ENVIRONMENT IN SPACE—v. 20

Edited by Gerhard B. Heller, NASA George C. Marshall Space Flight Center

The forty-five studies in this volume cover radiation properties of solids and their measurement, environment effects on thermal control coatings and their simulation, radiation characteristics of planetary bodies and results of flight experiments, identification of natural surfaces by remote sensing, thermal similitude and radiant heat transfer analysis of thermal systems, and heat transfer in the space environment.

Emissance, reflectance, and spectral emissance for a number of aerospace materials are presented, and special characteristics of a number of crystal solids are outlined. Standards and test equipment for determining such data are proposed. Several thermal control coatings are subjected to particle or electromagnetic space radiation, and their characteristics are presented. Flight test data for thermal control coatings are presented.

Other papers present thermal models for spacecraft interior temperatures, with specific applications of louvers, heat pipes, and other thermal protection systems, for both present and future projects.

975 pp., 6 x 9, illus. \$24.50 Mem. & List

TO ORDER WRITE: Publications Dept., AIAA, 1290 Avenue of the Americas, New York, N. Y. 10019